Influence of miR-34a on cerebral neuronal apoptosis in rats with cerebral ischemia reperfusion through the Notch1 signaling pathway

S.-P. WANG¹, D. WANG², H.-X. LI³, L. LIU⁴, X.-H. DUAN⁵

Suping Wang and Dong Wang contributed equally to this work

Abstract. – OBJECTIVE: To explore the influence and the underlying mechanism of micro-ribonucleic acid (miR)-34a on cerebral neuronal apoptosis in rats with cerebral ischemia-reperfusion (CIR).

MATERIALS AND METHODS: 60 adult male Wistar rats were randomly divided into 3 groups: Sham group, CIR group and miR-34a knockdown group. The rat model of CIR was established using the suture occlusion method. The expression level of miR-34a in lesion tissues in the three groups was determined via Reverse Transcription-Polymerase Chain Reaction (RT-PCR). The pathological injury of brain tissues was detected via hematoxylin-eosin (HE) staining and the infarction region in each group was evaluated via triphenyl tetrazolium chloride (TTC) staining. The terminal deoxynucleotidyl transferase-mediated dUTP nick end labeling (TUNEL) staining was performed to measure the cerebral neuronal apoptosis level. The level of Nissl's body in each group was detected via Nissl's staining. The expression level of the platelet-derived neurotrophic factor (PDNF) and Notch1/hypoxia-inducible factor-1a (HIF-1a) signaling pathway-related proteins in brain tissues were detected via immunohistochemistry and Western blotting, respectively.

RESULTS: The expression level of miR-34a in brain tissues of the CIR group was significantly increased compared to that of the Sham group (p < 0.05). After the intervention with miR-34a, the infarction area of brain tissues was markedly reduced when comparing to the CIR group (p < 0.05). In addition, the results of HE staining and NissI staining revealed that CIR treatment led to edema in cerebral neurons, disorderly arranged

neurons, and remarkably decreased number of Nissl's bodies. However, miR-34a knockdown following CIR significantly alleviated the brain tissue injury and markedly increased the number of Nissl's bodies (p < 0.05). The results of TUNEL staining also indicated that miR-34a siR-NA could remarkably reverse the cerebral neuronal apoptosis caused by CIR in rats (p < 0.05). According to the immunohistochemical staining results, the expression of PDNF in brain tissues declined in the CIR group, while enhanced in the miR-34a siRNA group (p < 0.05). Furthermore, the Western blotting results manifested that miR-34a siRNA could up-regulate the Notch1 and HIF-1a protein expressions in brain tissues of CIR rats.

CONCLUSIONS: Our data demonstrated that the miR-34a knockdown could alleviate the brain tissue injury and neuronal apoptosis by activating the Notch1/HIF-1a signaling pathway CIR-treated rats.

Key Words:

MiR-34a, Cerebral ischemia-reperfusion, Notch1.

Introduction

Stroke is the fifth major cause of death in the United States and one of the top ten causes of death in the world¹. Cerebral ischemia, one of the most destructive types of stroke, accounts for 87% in the total and is characterized by high morbidity, disability and mortality rates². Currently, limited drugs are available to effectively

¹Department of Neurological Rehabilitation, the Third People's Hospital of Qingdao, Qingdao, China

²Anesthesia Teaching and Research Section, Heze Medical College, Heze, China

³Department of Anesthesiology, the People's Hospital of Zhangqiu Area, Jinan, China

⁴EEG Room, the People's Hospital of Zhangqiu Area, Jinan, China

⁵Department of Anesthesiology, Jining No. 1 People's Hospital, Jining, China

improve the sequelae of cerebral ischemia with unsatisfied efficacy. Thrombolysis using the tissue plasminogen activator (tPA) is an effective therapeutic measure for stroke³. However, due to the short time window of tPA (only 6 h), the cerebral infarction patients who fail to undergo the treatment in time have poor prognosis⁴. Furthermore, even if the thrombolysis is successful, the continuous reperfusion after ischemia usually causes secondary damage to brain tissues, which is known as the cerebral ischemia-reperfusion (CIR) injury⁵. Therefore, clarifying the mechanism of the occurrence and development of CIR and searching the key targets are of great importance for the early prevention and precise treatment of CIR. Micro-ribonucleic acids (miRNAs) are a group of single-stranded non-coding RNAs with 20-24 nt in length and are widely existed in eukaryotes⁶. MiRNAs can regulate the expression of a variety of genes by targeted binding to specific genes, thus playing important roles in a variety of physiological activities, such as cell proliferation, differentiation and apoptosis⁷. For example, the inhibition of miR-155 significantly improved the neurological impairment in rats with cerebral infarction, reduced the volume of cerebral infarction and effectively promoted the angiogenesis in the ischemic region. The above effect might be mediated via the angiotensin type 1 receptor/ vascular endothelial growth factor receptor 2 (AT1R/VEGFR2) pathway⁸. It is also reported that decreased miR-195 markedly enhanced the angiogenesis in the ischemic area by up-regulating the expression of vascular endothelial growth factor A (VEGF-A)9. However, the role of miR-34 in neuronal apoptosis after CIR has not been reported. In this work, the rat model of CIR was established to observe the influence of miR-34a knockdown on neuronal apoptosis caused by CIR in rats. The underlying mechanism of miR-34a in CIR was then explored.

Materials and Methods

Animal Grouping and Modeling

A total of 60 male Wistar rats aged 12-14 weeks and weighing (85.32 ± 7.61) g were randomly divided into 3 groups using a random number table: Sham group (n = 20), CIR group (n = 20) and miR-34a siRNA group (n = 20). There were no significant differences in the initial week age and body weight among the three groups. MiR-34a siRNAs

were injected to rats via caudal vein for 2 consecutive days. The CIR operation was performed as follows: 1) the rats were anesthetized and fixed. 2) The left common carotid artery and vagus nerve were separated. 3) The proximal ends of the left common carotid artery and external carotid artery were ligated. 4) The distal end of the left common carotid artery was threaded and knotted in a slip knot. 5) The internal carotid artery was separated, and an incision was made in the proximal end of the internal carotid artery. 6) The wire was inserted into the incision and pushed forward for 18 mm till significant resistance, proving that the top of wire has reached the middle cerebral artery. 7) After 30 min, the wire was removed, followed by reperfusion. 8) The incision was sutured and disinfected. After 2 d, the score was given and the sample was taken. All animal operations were approved by the Animal Ethics Committee of Jining First People's Hospital.

Detection of Expression of Apoptosis-Related Genes Via Reverse Transcription-Polymerase Chain Reaction (RT-PCR)

The total RNA was extracted from cells using the TRIzol method (Invitrogen, Carlsbad, CA, USA). The concentration and purity of RNA were measured using an ultraviolet spectrophotometer, and the RNA with absorbance A_{260}/A_{280} of 1.8-2.0 was considered qualified. The messenger RNA (mRNA) was synthesized into the complementary deoxyribonucleic acid (cDNA) through RT and stored in the refrigerator at -80°C. RT-PCR system was prepared as follows: $2.5 \mu L$ $10 \times Buf$ fer, 2 µL cDNAs, 0.25 µL forward primers (20 μmol/L), 0.25 μL reverse primers (20 μmol/L), 0.5 μL dNTPs (10 mmol/L), 0.5 μL Taq enzymes $(2\times10^6 \text{ U/L})$ and 19 μL ddH₂O. The amplification system of RT-PCR was the same as above. The primer sequences used in this study were as follows: miR-34a, F: 5'-TTAGAACCAGTCCT-TACTC-3', R: 5'-CATTGATGTGTGGAGGA-3'; U6: F: 5'-GCTTCGGCAGCACATATACTA-AAAT-3', R: 5'-CGCTTCAGAATTTGCGTGT-CAT-3'.

Detection of Protein Expression Via Western Blotting

The brain tissues of rats in each group were fully ground in the lysis buffer, followed by ultrasonic lysis. Then, the lysis buffer was centrifuged, and the supernatant was taken and placed into the Eppendorf (EP) tube (Eppendorf, Hamburg, Germany). The protein concentration was detected via ultraviolet spectrometry, and the protein samples were quantified to be the same concentration. The protein was sub-packaged and placed in the refrigerator at -80°C. The sodium dodecyl sulfate-polyacrylamide gel electrophoresis (SDS-PAGE) was used to separate the protein samples. After being transferred onto a polyvinylidene difluoride (PVDF) membrane (Millipore, Billerica, MA, USA), the proteins were incubated with the primary antibody at 4°C overnight, and then incubated again with the goat anti-rabbit secondary antibody at room temperature for 1 h. The protein band was scanned and quantified using the Odyssey scanner. Glyceraldehyde-3-phosphate dehydrogenase (GAPDH) was selected as the internal reference.

Triphenyl Tetrazolium Chloride (TTC) Staining

The fresh brain tissues were placed into the grinding tool of brain tissue sections in the refrigerator at -20°C for 30 min and then sliced into 2 mm-thick sections (not more than 6 sections for each tissue). The sections were placed in fresh TTC solution (2%) (Oxoid, Hampshire, UK) for 30 min. After that, the sections were taken out, fixed with 4% paraformaldehyde and photographed.

Hematoxylin Eosin (HE) Staining

The brain tissues obtained in each group were placed in 10% formalin overnight, and then dehydrated and embedded in paraffin. Then, all brain tissues were sliced into 5 µm-thick sections, fixed on a glass slide and baked dry. The staining procedures were performed according to the instructions. Briefly, the sections were soaked in xylene, ethanol in gradient concentration and hematoxylin, respectively, and sealed with resin. After drying, the morphology of neurons was observed and photographed under a light microscope.

Terminal Deoxynucleotidyl Transferase-Mediated dUTP Nick End Labeling (TUNEL) Staining

The brain tissue sections were baked in an oven at 60°C for 30 min, deparaffinized with xylene (5 min, 3 times), and dehydrated with 100% ethanol, 95% ethanol and 70% ethanol 3 times. Then, the sections were incubated with protein kinase K for 0.5 h, washed with Phosphate-Buffered Saline (PBS), reacted with the terminal deoxynucleotidyl transferase (TdT) and Luciferase-labeled

dUTP at 37°C for 1 h. The sections were then incubated again with the horseradish peroxidase (HRP)-labeled specific antibody in an incubator at 37°C for 1 h, followed by reaction with diaminobenzidine (DAB; Solarbio, Beijing, China) as the substrate at room temperature for 10 min. The nucleus was stained with hematoxylin, followed by photography and counting under a fluorescence microscope.

Immunohistochemical Staining

The brain tissue sections were baked in the oven at 60°C for 30 min, deparaffinized with xylene (5 min \times 3 times), and dehydrated with 100% ethanol, 95% ethanol and 70% ethanol 3 times. Then, the endogenous peroxidase activity was inhibited with 3% hydrogen peroxide methanol. The tissues were sealed with goat serum for 1 h, incubated with the anti-platelet-derived neurotrophic factor (PDNF) antibody (diluted at 1:200 with PBS) at 4°C overnight. After being washed with PBS 4 times on a shaker, the secondary antibody was added, and the color was developed using diaminobenzidine. Totally 6 samples were randomly selected in each group and 5 fields of view were randomly selected in each sample, followed by photography under the light microscope $(200\times \text{ and } 400\times)$.

Nissl Staining

The paraffin or frozen sections were dehydrated with xylene, absolute ethanol, 95% alcohol, 80% alcohol, 70% alcohol and distilled water (the specific time could be based on HE staining) successively. Then, the sections were stained with 1% cresyl violet or 1% thionine for 10 min to 1 h, and washed with distilled water. After color separation with 70% alcohol, the sections were dehydrated with 70% alcohol, 80% alcohol and 95% alcohol for 2 min, respectively. The sections were dehydrated again with absolute alcohol twice (5 min/time) and xylene twice (10 min/time), and sealed with Permount Mounting Medium.

Statistical Analysis

Statistical Product and Service Solutions (SPSS) 22.0 software (IBM, Armonk, NY, USA) was used for the analysis of all data. Measurement data were expressed as mean \pm standard deviation, and t-test was used for the comparison of data between the two groups. p< 0.05 suggested that the difference was statistically significant.

Results

Expression of MiR-34a in Brain Tissues in Each Group

The RT-PCR results revealed that the miR-34a expression was markedly up-regulated in brain tissues in the CIR group compared with that in the Sham group (p < 0.05). After miR-34a knockdown, the expression miR-3 of 4a in brain tissues was markedly inhibited (p < 0.05) (Figure 1), indicating that the rat model of miR-34a knockdown was successfully established.

HE Staining Results of Brain Tissues in Each Group

The hippocampus structure in brain tissues was relatively complete and the cytoplasm was lightly stained and uniform in the Sham group and miR-34a siRNA group compared with that in the CIR group. In the CIR group, the cerebral neuronal structure was not complete anymore, and there were pathological changes, such as edema, nuclear displacement and cell necrosis (Figure 2).

Nissl Staining Results

As shown in Figure 3, the Nissl's bodies in brain tissues in each group were stained. The results showed that the number of Nissl's bodies had statistically significant differences among the three groups $[(62.33\pm2.93)\ vs.\ (18.39\pm1.93)\ vs.\ (45.34\pm2.91)]\ (p<0.05)$, indicating that the inhibition of miR-34a effectively attenuated the decline in Nissl's bodies induced by CIR.

TTC Staining Results

As shown in Figure 4, the area of cerebral infarction in each group was evaluated *via* TTC

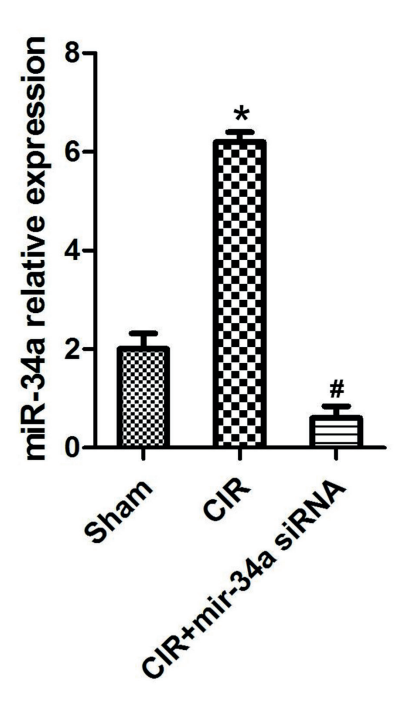


Figure 1. Expression of miR-34a in brain tissues in each group. Sham group: Sham-operation group; CIR group: cerebral ischemia-reperfusion group; miR-34a siRNA group: miR-34a knockdown group. * $p < 0.05 \ vs$. Sham group, # $p < 0.05 \ vs$. CIR group.

staining. The results manifested that the area of cerebral infarction was about $(45.37\pm9.38)\%$ in CIR group, while it declined to $(21.45\pm2.49)\%$ after miR-34a knockdown (p < 0.05).

Influence of MiR-34a Knockdown on Cerebral Neuronal Apoptosis in Each Group

The cerebral neuronal apoptosis in each group was quantified using TUNEL staining. It was

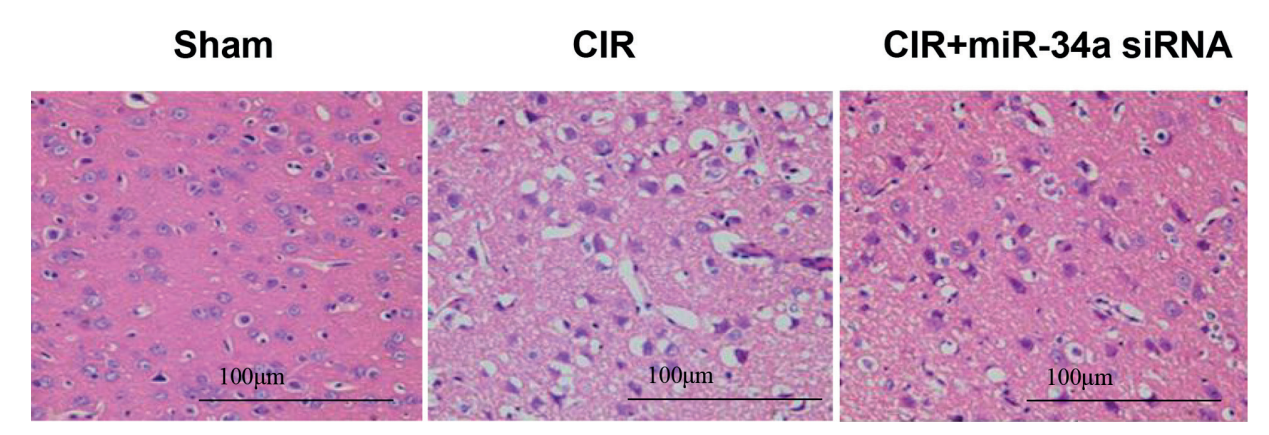


Figure 2. HE staining of brain tissues in each group. Sham group: Sham-operation group; CIR group: cerebral ischemia-reperfusion group; miR-34a siRNA group: miR-34a knockdown group. *p < 0.05 vs. Sham group, #p < 0.05 vs. CIR group.

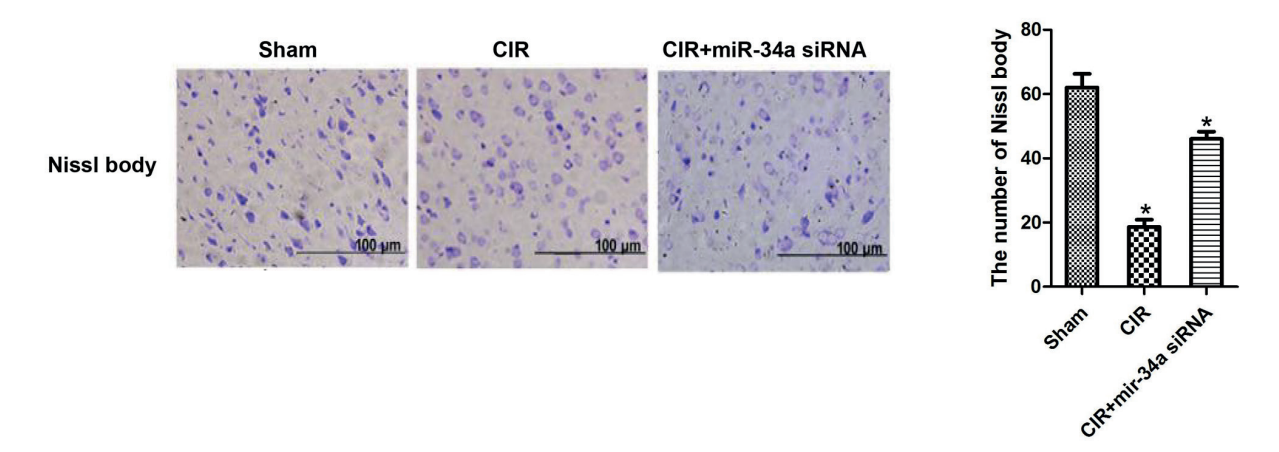


Figure 3. Nissl staining results in each group. Sham group: Sham-operation group, CIR group: cerebral ischemia-reperfusion group, miR-34a siRNA group: miR-34a knockdown group. * $p < 0.05 \ vs$. Sham group, # $p < 0.05 \ vs$. CIR group.

found that the number of apoptotic neurons was remarkably increased in the CIR group compared with that in the Sham group (p<0.05), while the neuronal apoptosis was also inhibited after miR-34a was decreased (p<0.05) (Figure 5).

Influence of MiR-34a Knockdown on Expression of PDNF in Brain Tissues

Moreover, the expression of PDNF in the brain tissues in each group was detected *via* immunohistochemistry. We found that, compared with the Sham group, the expression of PDNF in the CIR

group was markedly inhibited, which was then up-regulated after miR-34a knockdown (Figure 6).

Influence of MiR-34a Knockdown on the Expression of Notch1/HIF-10. in Each Group

Furthermore, the expression level of the Notch1/HIF-1 α signaling pathway in brain tissues in each group was detected *via* Western blotting. As shown in Figure 7, the Notch1/HIF-1 α signaling pathway was significantly suppressed in the CIR group compared with that in the Sham

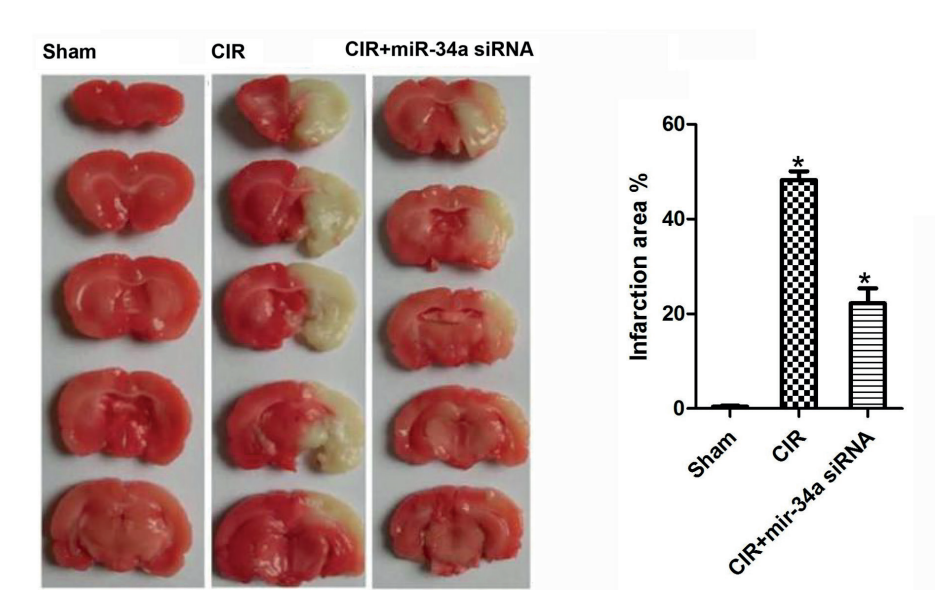


Figure 4. TTC staining results of brain tissues in each group. Sham group: Sham-operation group, CIR group: cerebral ischemia-reperfusion group, miR-34a siRNA group: miR-34a knockdown group. *p < 0.05 vs. Sham group, #p < 0.05 vs. CIR group.

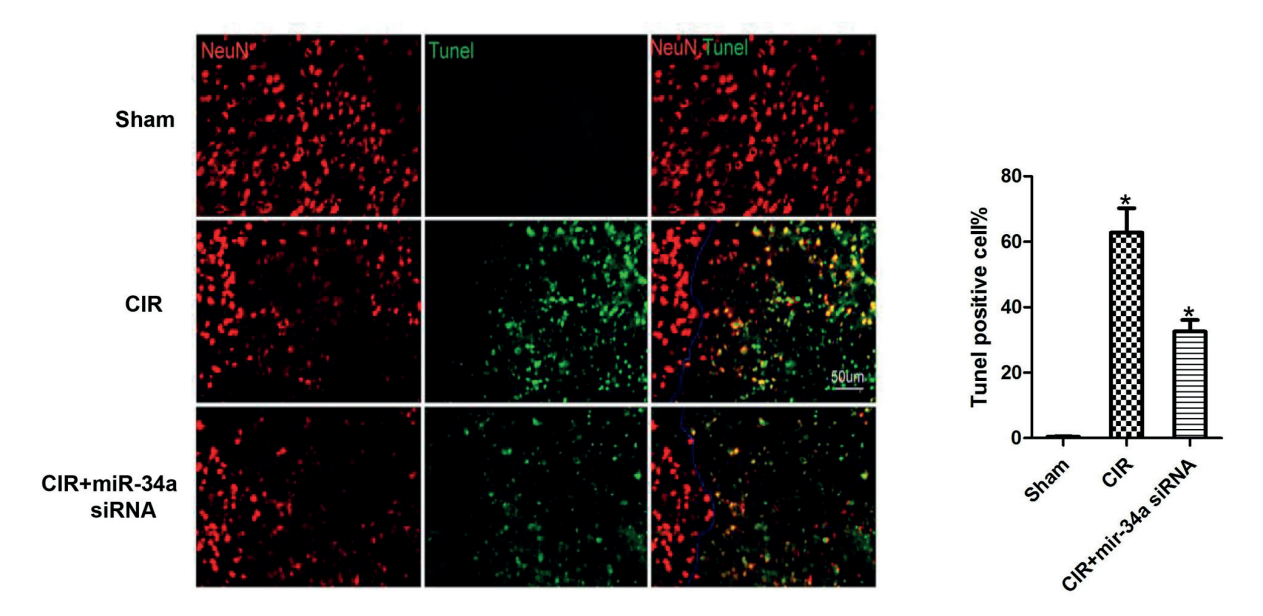


Figure 5. TUNEL staining results of brain tissues in each group. Sham group: Sham-operation group, CIR group: cerebral ischemia-reperfusion group, miR-34a siRNA group: miR-34a knockdown group (magnification: $40\times$). * $p < 0.05 \ vs$. Sham group, # $p < 0.05 \ vs$. CIR group.

group (p < 0.05). However, miR-34a knockdown reversed the CIR-induced decrease of Notch1 and HIF-1 α in brain tissues (p < 0.05).

Discussion

Cerebral infarction is currently one of the most common cerebrovascular diseases in the world¹⁰. It is reported that the morbidity and mortality rates of cerebral infarction showed an increasing trend year by year in western countries, especially the United States^{11,12}. The oc-

currence and development of cerebral infarction are closely related to genetic changes¹³. With the development of modern molecular biology and bioinformatics, more and more genes, RNAs and proteins have been proved to be involved in the pathogenesis of cerebral infarction¹⁴. According to current studies, neuronal apoptosis plays a crucial role in CIR injury, and the apoptosis level directly determines the severity degree and prognosis of this disease. In addition, oxidative stress, inflammation, mitochondrial dysfunction, Ca²⁺ overload and abnormal autophagy have close correlations with CIR injury^{15,16}. The Notch

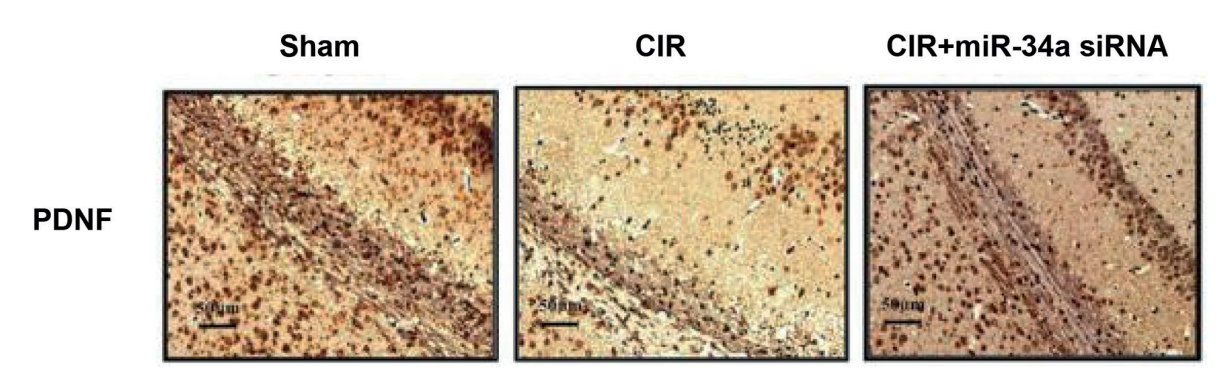


Figure 6. PDNF immumohistochemical staining results of brain tissues in each group. Sham group: Sham-operation group, CIR group: cerebral ischemia-reperfusion group, miR-34a siRNA group: miR-34a knockdown group group (magnification: $200 \times$). * $p < 0.05 \ vs$. Sham group, # $p < 0.05 \ vs$. CIR group.

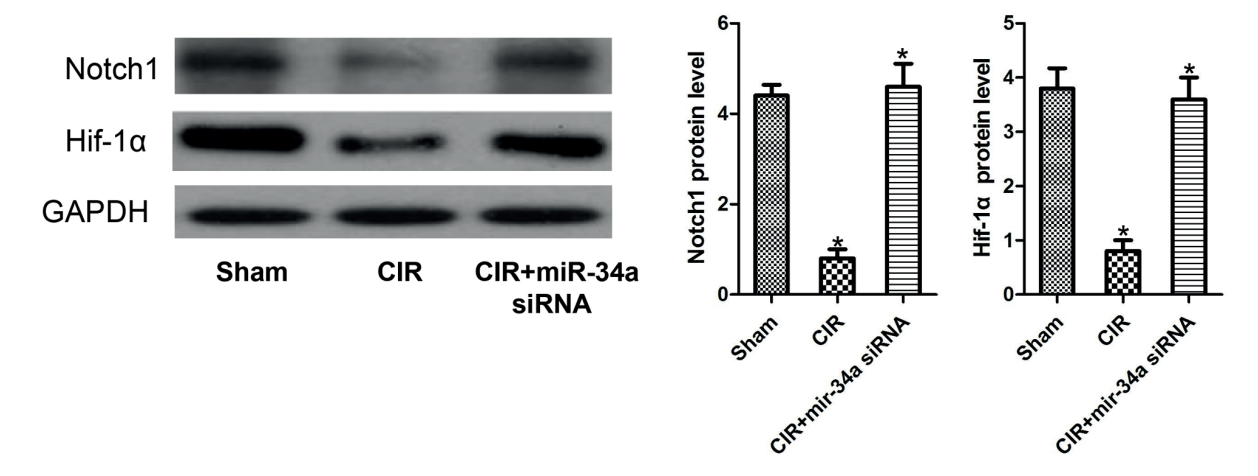


Figure 7. Notch1 and HIF-1 α protein expressions in brain tissues in each group. Sham group: Sham-operation group, CIR group: cerebral ischemia-reperfusion group, miR-34a siRNA group: miR-34a knockdown group. * $p < 0.05 \ vs$. Sham group, # $p < 0.05 \ vs$. CIR group.

family is a kind of highly-conserved cell membrane receptor proteins¹⁷. In mammals, there are mainly 4 members in the Notch family (Notch1, Notch2, Notch3 and Notch4)¹⁸. In fact, Notch is a kind of transmembrane protein containing both intracellular and extracellular domains¹⁹. When the ligand binds to the extracellular domain of Notch, the intracellular domain can be activated through twice hydrolysis by the TNF- α invertase and y-secretase. Then, the activated Notch intracellular domain (NICD) is subjected to nuclear translocation, enters the nucleus and binds to related transcription factors, initiating the expression of downstream genes²⁰. Zheng et al²¹ have demonstrated that Notch1 is highly expressed in neural stem cells and exert the function of regulating the neurodevelopment and morphology of dendritic cells. In addition, the Notch1 signaling pathway has a certain effect of nerve repair and is often activated in the case of ischemia hypoxia²². After ischemic stroke, the activated Notch1 can promote proliferation and differentiation of neuronal progenitor cells²³. According to animal experiments, the activation of the Notch1 signaling pathway can facilitate nerve regeneration in the ventricle, while the silencing of Notch1 can inhibit the proliferation of ependymal cells²⁴. He et al²⁵ have also argued that activating the Notch1 signaling pathway can promote the activation of macrophages and benefit the differentiation of dendritic cells, thereby alleviating the brain tissue injury caused by stroke. Notch1 has been reported to activate microglia, thus re-

ducing the inflammation in CIR lesion region and eliminating the damaged neurons²⁶. In addition, studies have revealed that the expression of Notch1 is regulated by miR-34a. For example, miR-34a reduced the invasion of cancer cells through targeted inhibition on Notch1 and Jagged1 in cervical cancer and choriocarcinoma²⁷. In glioma cells, the proliferation of glioma cells is significantly inhibited after the up-regulation of miR-34a, which might be related to the targeted inhibition of miR-34a on Notch128-31. In this work, the specific pathogen-free Wistar rats were used to successfully establish the rat model of miR-34a knockdown. The wire was inserted from the carotid artery to embolize the middle cerebral artery, thus better simulating the pathogenetic process of cerebral ischemia. Then, the wire was removed to promote the reperfusion process in rats. It was revealed for the first time in this study that the expression level of miR-34a was remarkably increased during the pathogenetic process of CIR. Inhibiting the miR-34a expression could effectively alleviate the CIR-induced cerebral injury, reduce the area of cerebral infarction, increase the number of Nissl's bodies, decrease the number of apoptotic cells in the lesion region, and up-regulate the expression level of PDNF. The mechanism of miR-34a siRNA in inhibiting CIR-induced cerebral injury might be related to the activation of the Notch1 signaling pathway by miR-34a siRNA. However, there were still some limitations in this study. (1) The cell experiments were not designed for verification. (2) The Notch1 inhibition assay was not designed. (3) Whether the direct target of miR-34a is Notch1 was not described.

Conclusions

MiR-34a knockdown played a protective role in the CIR injury in rats by activating the Notch1/ HIF-1α signaling pathway.

Conflict of Interests

The Authors declare that they have no conflict of interests.

References

- WANG J, CAO B, HAN D, SUN M, FENG J. Long non-coding RNA H19 induces cerebral ischemia reperfusion injury via activation of autophagy. Aging Dis 2017; 8: 71-84.
- ZENG X, WANG H, XING X, WANG Q, LI W. Dexmedetomidine protects against transient global cerebral ischemia/reperfusion induced oxidative stress and inflammation in diabetic rats. PLoS One 2016; 11: e151620.
- FENG J, CHEN X, GUAN B, LI C, QIU J, SHEN J. Inhibition of peroxynitrite-induced mitophagy activation attenuates cerebral ischemia-reperfusion injury. Mol Neurobiol 2018; 55: 6369-6386.
- CHANG C, ZHAO Y, SONG G, SHE K. Resveratrol protects hippocampal neurons against cerebral ischemia-reperfusion injury via modulating JAK/ERK/STAT signaling pathway in rats. J Neuroimmunol 2018; 315: 9-14.
- Lou Z, Wang AP, Duan XM, Hu GH, Song GL, Zuo ML, Yang ZB. Upregulation of NOX2 and NOX4 mediated by TGF-beta signaling pathway exacerbates cerebral ischemia/reperfusion oxidative stress injury. Cell Physiol Biochem 2018; 46: 2103-2113.
- SHISHODIA G, VERMA G, DAS BC, BHARTI AC. miRNA as viral transcription tuners in HPV-mediated cervical carcinogenesis. Front Biosci (Schol Ed) 2018; 10: 21-47.
- SEOK H, LEE H, JANG ES, CHI SW. Evaluation and control of miRNA-like off-target repression for RNA interference. Cell Mol Life Sci 2018; 75: 797-814.
- MENG YC, DING ZY, WANG HQ, NING LP, WANG C. Effect of microRNA-155 on angiogenesis after cerebral infarction of rats through AT1R/VEGFR2 pathway. Asian Pac J Trop Med 2015; 8: 829-835.
- ZHAO WJ, ZHANG HF, SU JY. Downregulation of microRNA-195 promotes angiogenesis induced by cerebral infarction via targeting VEGFA. Mol Med Rep 2017; 16: 5434-5440.

- Bong JB, Kang HG, Choo IS. Acute cerebral infarction after pyrethroid ingestion. Geriatr Gerontol Int 2017; 17: 510-511.
- ZHANG C, ZHAO S, ZANG Y, GU F, MAO S, FENG S, HU L, ZHANG C. The efficacy and safety of DI-3n-butylphthalide on progressive cerebral infarction: a randomized controlled STROBE study. Medicine (Baltimore) 2017; 96: e7257.
- 12) HE X, LI DR, CUI C, WEN LJ. Clinical significance of serum MCP-1 and VE-cadherin levels in patients with acute cerebral infarction. Eur Rev Med Pharmacol Sci 2017; 21: 804-808.
- Qi X, Shao M, Sun H, Shen Y, Meng D, Huo W. Long non-coding RNA SNHG14 promotes microglia activation by regulating miR-145-5p/PLA2G4A in cerebral infarction. Neuroscience 2017; 348: 98-106.
- 14) Wang K, Zhang D, Wu J, Liu S, Zhang X, Zhang B. A comparative study of Danhong injection and Salvia miltiorrhiza injection in the treatment of cerebral infarction: a systematic review and meta-analysis. Medicine (Baltimore) 2017; 96: e7079.
- 15) Lu G, Wong MS, Xiong M, Leung CK, Su XW, Zhou JY, Poon WS, Zheng V, Chan WY, Wong G. Circulating microRNAs in delayed cerebral infarction after aneurysmal subarachnoid hemorrhage. J Am Heart Assoc 2017; 6: e005363.
- NANDAGOPAL N, SANTAT LA, LEBON L, SPRINZAK D, BRONNER ME, ELOWITZ MB. Dynamic ligand discrimination in the Notch signaling pathway. Cell 2018; 172: 869-880.
- LUBIN DJ, MICK R, SHROFF SG, STASHEK K, FURTH EE. The notch pathway is activated in neoplastic progression in esophageal squamous cell carcinoma. Hum Pathol 2018; 72: 66-70.
- 18) PAN Y, MAO Y, JIN R, JIANG L. Crosstalk between the Notch signaling pathway and non-coding RNAs in gastrointestinal cancers. Oncol Lett 2018; 15: 31-40.
- Li Q, Zhang X, Cheng N, Yang C, Zhang T. Notch1 knockdown disturbed neural oscillations in the hippocampus of C57BL mice. Prog Neuropsychopharmacol Biol Psychiatry 2018; 84: 63-70.
- 20) CHEN F, ZHANG L, WANG E, ZHANG C, LI X. LncRNA GAS5 regulates ischemic stroke as a competing endogenous RNA for miR-137 to regulate the Notch1 signaling pathway. Biochem Biophys Res Commun 2018; 496: 184-190.
- 21) ZHENG J, WATANABE H, WINES-SAMUELSON M, ZHAO H, GRIDLEY T, KOPAN R, SHEN J. Conditional deletion of Notch1 and Notch2 genes in excitatory neurons of postnatal forebrain does not cause neurodegeneration or reduction of Notch mRNAs and proteins. J Biol Chem 2012; 287: 20356-20368.
- CHENN A, McConnell SK. Cleavage orientation and the asymmetric inheritance of Notch1 immunoreactivity in mammalian neurogenesis. Cell 1995; 82: 631-641.
- 23) REDMOND L, OH SR, HICKS C, WEINMASTER G, GHOSH A. Nuclear Notch1 signaling and the regulation of dendritic development. Nat Neurosci 2000; 3: 30-40.

- 24) Hatakeyama J, Kageyama R. Notch1 expression is spatiotemporally correlated with neurogenesis and negatively regulated by Notch1-independent Hes genes in the developing nervous system. Cereb Cortex 2006; 16 Suppl 1: i132-i137.
- 25) HE W, LIU Y, TIAN X. Rosuvastatin improves neurite outgrowth of cortical neurons against oxygen-glucose deprivation via Notch1-mediated mitochondrial biogenesis and functional improvement. Front Cell Neurosci 2018; 12: 6.
- 26) Yang Y, Huang G, Zhang X, Liu H. [Effects of folio acid on neural cell apoptosis and Notch1 mRNA expression in rats with brain infarction]. Wei Sheng Yan Jiu 2008; 37: 671-674.
- 27) SONNEN KF, LAUSCHKE VM, URAJI J, FALK HJ, PETERSEN Y, FUNK MC, BEAUPEUX M, FRANCOIS P, MERTEN CA, AULE-HLA A. Modulation of phase shift between Wnt and Notch signaling oscillations controls mesoderm segmentation. Cell 2018; 172: 1079-1090.

- 28) ZHANG J, YU K, HAN X, ZHEN L, LIU M, ZHANG X, REN Y, SHI J. Paeoniflorin influences breast cancer cell proliferation and invasion via inhibition of the Notch1 signaling pathway. Mol Med Rep 2018; 17: 1321-1325.
- 29) REN C, YAO Y, HAN R, HUANG Q, LI H, WANG B, LI S, LI M, MAO Y, MAO X, XIE L, ZHOU L, HU J, JI X, JIN K. Cerebral ischemia induces angiogenesis in the peri-infarct regions via Notch1 signaling activation. Exp Neurol 2018; 304: 30-40.
- 30) PANG RT, LEUNG CO, YE TM, LIU W, CHIU PC, LAM KK, LEE KF, YEUNG WS. MicroRNA-34a suppresses invasion through downregulation of Notch1 and Jagged1 in cervical carcinoma and choriocarcinoma cells. Carcinogenesis 2010; 31: 1037-1044.
- 31) LI WB, MA MW, Dong LJ, WANG F, CHEN LX, LI XR. MicroRNA-34a targets notch1 and inhibits cell proliferation in glioblastoma multiforme. Cancer Biol Ther 2011; 12: 477-483.